Journal of
Applied Remote Sensing

RemoteSensing.SPIEDigitalLibrary.org

Thermal infrared anomaly indicating unformed strong earthquake sequences

Qinglin Yao
Zuji Qiang

SPIE.

Thermal infrared anomaly indicating unformed strong earthquake sequences

Qinglin Yao* and Zuji Qiang
Institute of Geology, China Earthquake Administration, P.O. Box 9803, Beijing 100029, China

Abstract. By processing and analyzing many satellite remote sensing images in infrared channels, we found visual evidence indicating earthquake sequences. In a sequence, large earthquakes could migrate thousands of kilometers along a linear route from one land mass to another, and infrared anomalies also cover these land masses. The sequence has at least two types: (1) quakes alternately occurring at two ends of a belt, or (2) quakes progressively migrating along a far-flung route. The former can be foreshowed in a single infrared belt with a legible directed structure and higher brightness temperature; the latter can be identified in advance from the shift, veer, and deformation of more areas with a higher brightness temperature. The thermal infrared anomalies with a shorter duration are used to predict the quake-sequence evolving in a longer period. Two sorts of sequences can meet and form a more complex structure that can also be shown in advance by an anomalous infrared area. These studies on the seismic sequences will provide a potent means for analyzing earthquake-pregnant fields and estimating the location of unformed earthquake sequences.
[DOI: 10.1117/1.JRS.9.096089]

Keywords: earthquake sequence; precursor; thermal infrared; land surface temperature; image analysis.

Paper 14366 received Jul. 9, 2014; accepted for publication Dec. 17, 2014; published online Feb. 4, 2015.

1 Introduction

After a large earthquake occurs, people always hope to understand whether relevant strong events ($M \geq 6$) will sequentially transpire and—if so—where they will be. The occurrence of some strong events alters the earthquake-pregnant field and accelerates the generation of subsequent quakes in the interrelated regions. Such correlative earthquakes successively taking place form a so-called strong earthquake chain (ignoring the causality between earthquakes, we often call the chain a "sequence"). Past studies of the chain (sequence) have mainly focused on geological structures, crustal stress, strain field, plate movement, focal mechanism, and some statistical characteristics.[1–20] All these studies only indirectly speculated about the chains—whether two successive events indeed correlate lack direct evidence. In many situations, finding such evidence is difficult. If a technique can directly observe the sequence in advance, it will help us understand the sequence's authenticity, development law, and spatiotemporal distribution.

Satellite-based remote sensing observing the land surface temperature was considered for the following properties: (1) some of the observed temperature alteration was closely related to impending strong events;[21] (2) a vast region can be observed simultaneously; (3) we have the image data for all the areas of which we are interested; (4) the observation can be done automatically and accurately; (5) smaller ground temperature changes (e.g., <1 K) can be distinguished; and (6) the satellites we used can repeatedly observe the same location in a short time interval (0.5 h).

Since 1989, we have observed brightness temperature anomalies from the infrared images before many imminent earthquakes and effectively extracted the seismic predictive information.[22,23] Around 2010, we found that the thermal infrared (TIR) images could not only prefigure

*Address all correspondence to: Qinglin Yao, E-mail: qlnh@sohu.com
0091-3286/2015/$25.00

an impending single strong earthquake, but also synchronously reflect the evolution of a linked earthquake doublet.[24] After that, we found that a TIR calefactive field might be determined by more earthquakes in a larger scope and a longer time.[25] These successful studies preliminarily demonstrated the feasibility of studying strong earthquake sequences using satellite TIR images. Do TIR images contain more complex information of an earthquake sequence that extends longer distances and lasts longer? By analyzing TIR images and other data, Yao and Qiang[24] found that 2008 Yutian M_S 7.3 and Wenchuan M_S 8.0 events had a consecutive stress evolution background and a chained relationship. [M_S, m_L, m_b, and m_B (collectively called M) are magnitude that is calculated in different ways.] Did the chained sequence end at Wenchuan? If the two events are only a part of a long earthquake sequence, then where will the sequence extend to? Can other strong events in the sequence also be foreshowed by TIR images? Furthermore, we want to know whether TIR images can indicate other types of earthquake sequences and how TIR images foreshow various sequences. For this purpose, we processed many FY2-c infrared images and analyzed the structural correlations between abnormal surficial temperature variation and various factors associated with quakes in different sequences.

2 Seismic Precursors, Occurrence, and Disasters

Earthquakes are one of the worst natural disasters in the world. For example, on March 11, 2011, a magnitude 9.0 earthquake struck off the coast of Japan in the Tohoku region, resulting in a tsunami. The confirmed death toll was 15,884 as of February 10, 2014.[26] Material damage from the earthquake and tsunami is estimated to be about 25 trillion yen ($300 billion).[26]

Tectonic earthquakes are the most common type of earthquake that can cause the most serious disasters including heavy casualties and economic losses. The occurrence mechanism of a tectonic earthquake is illustrated through Fig. 1. The crust and the mantle are always in movement and are changing along with the action of force. A nonhomogeneous crust medium and uneven fault planes stop the movement at some places and form a region of stress locking. Hampered terranes accumulate stress and produce tectonic deformation, causing a series of physical and chemical changes. Those changes transmit their effects to the ground and can even radiate through the air to form a seismic precursory field [Fig. 1(a)]. When the stress concentration is large enough, the deformation will exceed the rock fracturing strength, the terranes will break and slip, the energy that accumulated long-term will be released quickly, and the seismic waves coming from rock vibrations will transmit to the ground with a great destructive effect [Fig. 1(b)].

Remote sensing has important uses in earthquake disaster reduction. In addition to observing abnormal TIR changes caused by seismogenic processes, it can also be used in other related fields,[27,28] particularly in the mapping and interpretation of active faults,[29] ground movement detection, coseismic deformations observation, and earthquake damage assessment.[30] High-resolution satellite images over the main affected areas can be acquired a few hours after a catastrophic seismic event occurrence.[31] Based on these remotely sensed data, rapid damage assessment can effectively support the emergency response activities carried out by the government and the humanitarian agencies. For example, after Haiti was hit by a devastating earthquake on January 12, 2010, this damage assessment helped the United Nations World Food Programme staff to deliver food to the hungry population in the quickest way.[31]

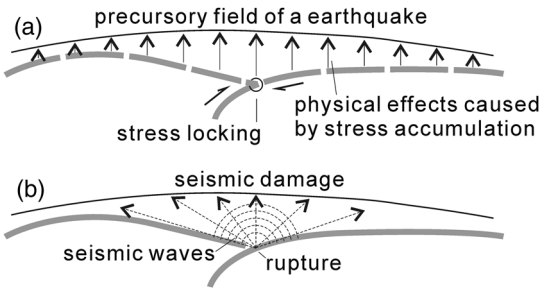

Fig. 1 Formation of the precursor field (a) and the occurrence of an earthquake (b).

3 Earthquake Sequence and Interrelated Thermal Infrared Analysis

In interrelated dynamic and tectonic environments, occurrences of some earthquakes correspond with certain spatiotemporal rules. These quakes can be characterized as a sequence or chain. The following rules enumerate the characteristics of a quake sequence (chain):

1. Strong quakes in a sequence occur relatively densely within a limited period. The time interval between the quakes has some pattern, e.g., longer intervals alternate with shorter ones.
2. Spatial distribution of strong earthquakes has a linear characteristic. In other words, the strong earthquakes usually migrate along a linear route or a very simple combination of linear routes. For instance, while analyzing the activity of quakes with $M \geq 7$ in China and its vicinity from 1979 to 1990, Yao found that the track of the strong quakes migrating in a year usually formed a simple geometric figure (such as triangle).[32]
3. The strong quakes occur in a certain order. For example, they gradually migrate to a distant place or occur several times in a small area within a few years before migrating elsewhere.
4. All earthquakes are larger than a lower limit value (such as M 6, M 7, or M 8) that is determined according to regional seismicity and research target.
5. The quakes in a sequence have a mutual earthquake-pregnant field or a combination of some interactive fields.

These characteristics are helpful for analyzing the location and occurrence time of the next strong quake in a sequence. Here, we mainly pay attention to two types of sequences. The first is that the strong quakes alternately occur at two ends of a belt; the second is that the strong quakes progressively migrate along a far-flung route and return after reaching the end of the route.

The main characteristic of the sequence hides in the TIR images' structures and variations. Nonuniform warming forms different brightness temperature layers and pieces. They make the TIR a combination of different areas, lines, and points (verges, endpoints, flex points, intersection, and so on). People should not waste time demonstrating whether or not this warming is a seismic precursor according to some theoretic seismic mechanism. As long as some areas, lines, and points accord with future epicenters, the TIR anomaly plays a virtual role in foreseeing quakes. The infrared anomaly indicating a seismic sequence often is an isolated elliptic uneven warming area (Figs. 2–7). It can step over different geological, geomorphologic, and tectonic units (Fig. 5) and has some special distribution property in azimuth, location, extent, and structures (Figs. 2–8). The warming range is not a very important index for identifying

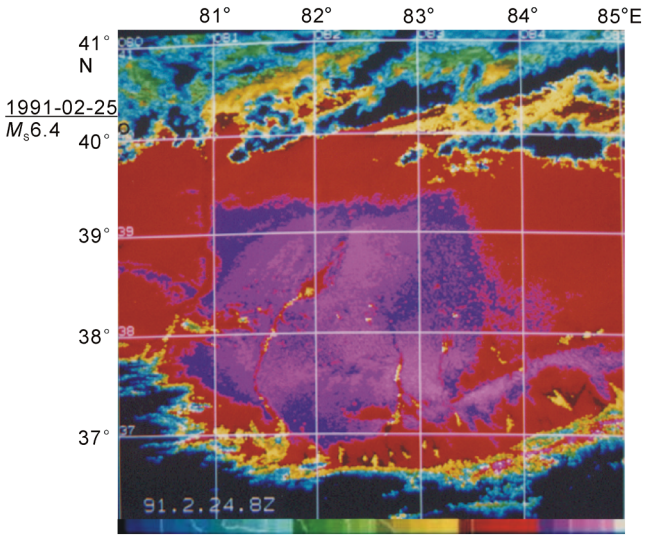

Fig. 2 TIR warming ellipse (1991-02-24T08:00, UTC is used in the whole paper) indicating Kelpin M_S 6.4 earthquake (February 25, 1991). Note: The brightness temperatures in the color code bar increase gradually from left to right.

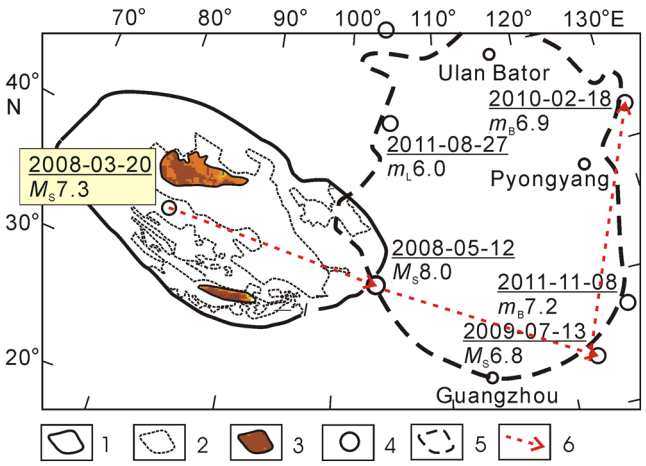

Fig. 3 Relationship between main seismic chain and branched one and between the chains and their TIR fields. Notes: 1—TIR warming ellipse (2008-03-07T13) that relates to two large earthquakes; 2—general elevated temperature area (2008-03-07T13); 3—higher elevated temperature area (2008-03-07T13); 4—epicenters; 5—TIR warming ellipse at 2008-03-19T06 that was jointly configured by the main seismic chain and the branched one; and 6—the track of earthquakes migrating; smaller circles are cities.

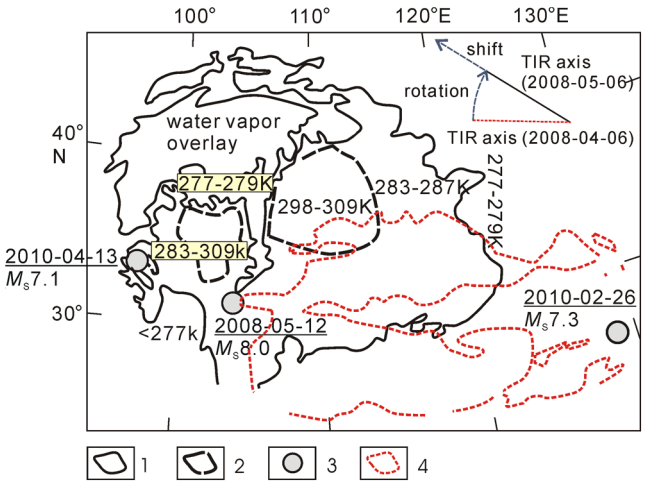

Fig. 4 Veer and backward shifts of TIR warming ellipse indicating earthquake sequence. Notes: 1—general earthquake-related elevated temperature area on May 6, 2008; 2—higher earthquake-related elevated temperature area on May 6, 2008; 3—epicenters; and 4—earthquake-related elevated temperature area on April 6, 2008.

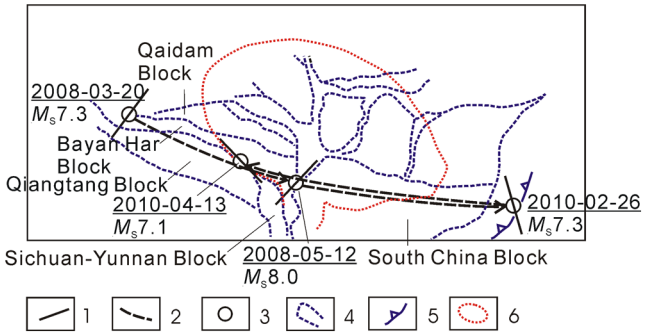

Fig. 5 Relationship among the Yutian–Ryukyu sequence, the causative faults, the TIR anomaly, and the active blocks. Notes: 1—causative faults; 2—route of migrating earthquakes in the Yutian–Ryukyu sequence; 3—epicenters; 4—active blocks; 5—plate boundary; and 6—TIR anomaly on May 6, 2008.

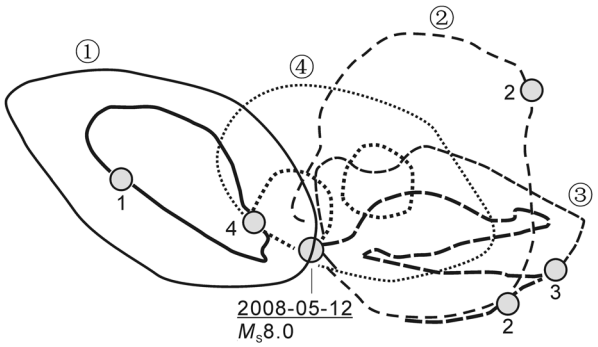

Fig. 6 Change in position and orientation of infrared zones indicating the earthquake sequence. Notes: The thicker lines sketch the contours of the areas with higher temperature within the TIR warming regions that have been outlined with a same line-style; ①–④ and 1–4 express the appearance order of infrared warming areas and earthquakes, respectively; two "2" belong to the same branched chain and same warming area, both were later than "1" and earlier than "3."

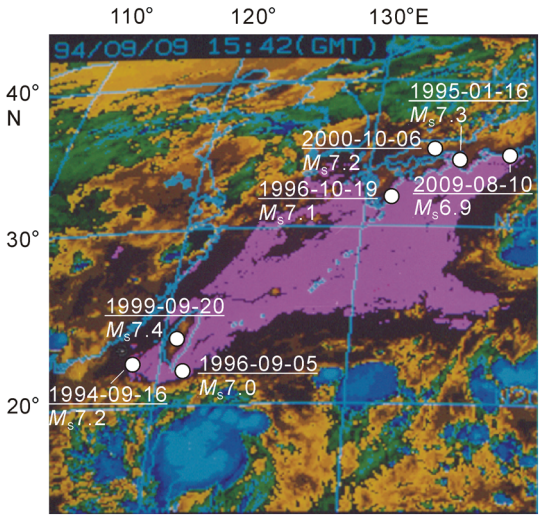

Fig. 7 TIR image (September 09, 1994) indicating T-H earthquake sequence.

a quake-related temperature field. All the warmings are possible as long as TIR images can show it. In a variety of quake cases, we found that a warming of more than 0.5 K could be related to quakes. Even some lower temperature zones (not warming or locally lowering temperature) with special structural and spatiotemporal characteristics may be a seismic precursor. The temperature may have complex changes inside a TIR anomaly body. The complexity of the TIR field's changes is determined by the nonlinear process of the strong earthquakes' gestation. TIR seismic precursors are the product of geostress change caused by the diastrophism and mantle movement. In the satellite remote sensing images, it was easy to find the trace of crustal stress action and the rotation and upwelling of the mantle agreeing with the focal mechanism solutions, tectonic analysis, and so on.

4 Thermal Infrared Images Indicating Yutian-Wenchuan Quake Sequence

The two previously mentioned large earthquakes, Yutian M_S 7.3 on March 20 and Wenchuan M_S 8.0 on May 12, occurred in western China in 2008. Some abnormal TIR areas showed the pertinent relation between the developing processes of the two events. For example, on March 7, 2008, an abnormal TIR ellipse had the following characteristics (Fig. 3):

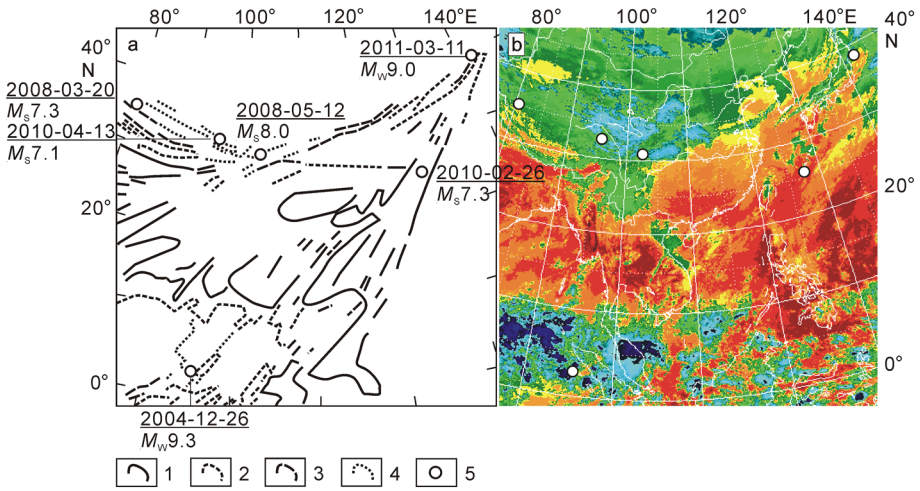

Fig. 8 Conjunct infrared structures analytic diagram (a) and original TIR image (b) (December 10, 2004) of two earthquake sequences. Notes: 1—the TIR linear structure (boundaries, strips, and so on) with brightness temperature (T_B; unit: K) more than 294; 2—$294 \geq T_B > 283$; 3—$283 \geq T_B > 275$; 4—$275 \geq T_B > 253$; and 5—epicenters.

1. The epicenter (35.64°N, 81.54°E) of the M_S 7.3 Yutian event was on the boundary of the inner higher warming area in the west-central part of the ellipse, rather than the boundary of the whole ellipse.
2. The warming ellipse extended east southeast (ESE), clearly inconsistent with the strike northeast (NE) of the seismogenic fault (Table 1).
3. The main linear structure within the ellipse was also oriented ESE.
4. The higher temperature was mainly distributed in the central and ESE sections of the ellipse.

The TIR ellipse was the precursor of the Yutian event; the ellipse's characteristics, however, had not shown a developing trend toward the Yutian epicenter. Instead, it was weighted toward the ESE of Yutian. It seemed to be a hint that an event larger than the Yutian's would be to ESE of Yutian. The hint was strengthened by the subsequent TIR evolution: all the TIR anomalies moved and deformed around the ESE end, like an axis, of the TIR ellipse on March 7. Later facts proved that these phenomena were relative to the Wenchuan 8.0 earthquake occurring at the ESE end (31.01°N, 103.42°E) of the ellipse (Fig. 3).

Before the Wenchuan earthquake occurrence, no matter how the thermal ellipse altered its area, shape, integrity, direction of rotation, position, and orientation, the ellipse boundaries would never lose contact with the Wenchuan epicenter. It was obvious that the Wenchuan epicenter could closely control the warming anomalies. On March 19, 2008, an unusual TIR

Table 1 Occurrence of a few seismogenic faults.

Epicentral location	Date	Magnitude (M_S)	Fault strike (deg)	Dip angle (deg)	Fault property
Yutian	March 20, 2008	7.3	203	52	Nss
Wenchuan	May 12, 2008	8.0	231	35	Td
Ryukyu	February 26, 2010	7.3	0	81	Dst
Yushu	April 13, 2010	7.1	300	88	Sst

Notes: Seismogenic faults data were obtained from the Global CMT Catalog of Harvard and some megaseism's special topics in the websites of China Earthquake Administration and United States Geological Survey; magnitudes are according to China Seismic Networks (CSN). Nss means the normal fault with small sinistral strike-slip component; Td means the thrust and dextral strike-slip; Dst means the dextral strike-slip with small thrust component; and Sst means the sinistral strike-slip with some thrust component.

alteration caught our attention; the calefactive ellipse moved a great distance way (thousands of kilometers) from the west northwest (WNW) side of the Wenchuan epicenter to its ESE side. Almost no single earthquake can vary its infrared precursor in this way. The location and direction of the isolated warming ellipses of a single earthquake must have steadier relations with the epicenter, seismogenic zone, and causative fault. However, just as two points can determine a line, two strong earthquakes can determine the orientation of the infrared regions, which is irrelevant to the seismogenic structures of either event. As a representative example, the TIR precursor of the Yutian and Wenchuan events was in the ESE direction which corresponded to the line connecting the two epicenters (Fig. 3). More than three earthquakes can control the range of a warming area.[25] Therefore, just as the warming ellipse that was jointly determined by the earthquake doublet at Yutian and Wenchuan was located on the WNW side of Wenchuan, the warming ellipses that moved to the ESE of Wenchuan should also mean that other strong earthquakes to the ESE of Wenchuan will be chained in the next few years.

5 Thermal Infrared Anomaly Affected by a Branched Chain

Before the Wenchuan 8.0 earthquake occurrence, the shape, fine structure, and movement of the infrared warming ellipses had a total orientation ESE, which was also the direction of the strong earthquake sequence (chain). The warming ellipse's extension direction, however, unexpectedly turned into north northeast (NNE) on March 19 (Fig. 3). This must be due to the effect from some future strong earthquakes outside the aforementioned sequence.

Table 2 Some earthquakes in the branched chain.

Date	Latitude (deg)	Longitude (deg)	Magnitude
November 08, 2011	27.20	125.90	m_B 7.2
August 27, 2011	44.02	104.58	m_L 6.0
May 10, 2011	43.30	131.20	m_b 6.1
April 16, 2011	25.30	124.15	m_B 6.0
March 04, 2010	22.96	120.70	M_S 6.7
February 18, 2010	42.73	130.91	m_B 6.9
December 19, 2009	23.88	121.64	M_S 6.6
November 05, 2009	23.84	120.70	m_L 6.0
October 03, 2009	23.76	121.57	M_S 6.2
July 13, 2009	24.09	122.23	M_S 6.8
August 27, 2008	51.66	104.28	M_S 6.4
May 19, 2008	42.56	131.87	m_b 6.0
May 13, 2008	30.95	103.42	M_S 6.1
May 12, 2008	31.26	103.67	M_S 6.3
May 12, 2008	31.26	103.59	m_B 6.2
May 12, 2008	31.27	103.82	M_S 6.3
May 12, 2008	31.01	103.42	M_S 8.0
April 23, 2008	22.96	121.74	M_S 6.4

Notes: Data come from the CSN earthquake catalog.
M_S—surface wave magnitude, m_B—long-periodic body wave magnitude, m_b—short-period body wave magnitude, m_L—near earthquake magnitude.

Later, we discovered such strong earthquakes formed a branched chain (shorter chain stretching from a main chain to another place). They occurred more than 3 years later and controlled the shape, position, and direction of the TIR ellipse together with the Wenchuan 8.0 event (Fig. 3 and Table 2). Regardless of the strong events on the west border of the warming ellipse, which made earthquake migration more complex, the strong events only on the NNE trending east border migrated back and forth several times. They are an M_S 6.4 quake on April 23, 2008, at the south end of the TIR warming area (this is abbreviated to S); m_b 6.0, May 19, 2008 (N); M_S 6.2 to 6.8, from July 13 to December 19, 2009 (S); m_B 6.9, February 18, 2010 (N); M_S 6.7, March 4, 2010 and m_B 6.0, April 16, 2011 (S); m_b 6.1, May 10, 2011 (N); and m_B 7.2, November 8, 2011 (S).

From Fig. 3, we can see that the directions of the TIR ellipses and the migration of the earthquakes both had obvious turns. The M_S 6.8 quake on July 13, 2009, in the NNE-extending shorter chain was also in the ESE-extending main chain. Therefore, the shorter chain did not exist independently but was a branched chain. The two chains formed a sort of compound chain. The NNE-extending ellipse was a joint product of the main chain, the branched chain, and the TIR reinforcement effect of the impending Wenchuan 8.0 event.

6 Further Changes of the Warming Areas Indicating the Main Chain's Development

The warming ellipse did not always turn to NNE, but soon turned back to ESE and was still on the east side of Wenchuan. For example, on April 6, a TIR anomaly extended from Wenchuan to the East China Sea. This change must have a reason. The ESE must have some sites gestating other earthquakes which might not yet have revealed clear signs. Sure enough, on the edge of the curved fine structure growing in the foreside of the newborn warming ellipse Ryukyu Islands (25.86°N, 128.65°E), an M_S 7.3 earthquake took place on February 26, 2010 (Fig. 4). The TIR warming area from Wenchuan to Ryukyu was a direct indication of the relationship between the two quakes.

Six days before the Wenchuan 8.0 Earthquake, viz. on May 6, 2008, the TIR warming ellipse obviously changed its position and configuration again. The ellipse still retained its ESE strike, but moved to the NE of the Wenchuan epicenter. The large warming ellipse included two cores whose principal parts had higher temperatures (Fig. 4). From Fig. 4, we can see that the western and the southwestern sides of the TIR ellipse on May 6 and the southern side of the TIR ellipse on April 6 linked into an arc showing the affinity of both ellipses toward seemingly natural transitions. The shift of the elliptical TIR anomalies from the position on April 6 to that on May 6, however, needed a rotation of about 28 deg and a backward movement of about 900 km. Do these changes have any special meaning? The answer to the question did not appear until nearly 2 years later. From the Yutian M_S 7.3 event, via Wenchuan M_S 8.0, to Ryukyu M_S 7.3, it was a catenulate sequence moving ESE step-by-step. More than 1 month after reaching Ryukyu, the quake chain returned to the WNW; an M_S 7.1 event occurred at Yushu (33.22°N, 96.59°E) to the WNW of Wenchuan on April 13, 2010. The Yushu event was located just on the southwest (SW) edge of the aforementioned TIR warming ellipse of May 6, 2008, and on a corner of a core within the ellipse (Fig. 4). It is obvious that every transformation of the isolated TIR ellipses was determined by the earthquake sequence.

The Yutian, Wenchuan, Ryukyu, and Yushu quakes formed an ESE strike sequence (it is abbreviated to Yutian–Ryukyu sequence or Y–R chain). In the sequence, the time interval between the Yutian event and the Wenchuan event was more than 1 month (52 days) in 2008 and between the Ryukyu event and the Yushu event was also more than 1 month (46 d) in 2010. Two earthquake doublets in 2008 and 2010 similarly spanned another epicenter in the sequence (Fig. 5). Therefore, the sequence had an approximately symmetrical structure of bidirectional migration.

7 Earthquake Sequence Traversing Crustal Blocks

No fault runs through different strong earthquakes in the Yutian–Ryukyu sequence. Moreover, the sequence traverses different tectonic blocks Bayan Har, Qiangtang, Sichuan-Yunnan,

southern China and is diagonal to some of their boundary faults. Strikes of the causative faults in the sequence are inconsistent with the sequence (Fig. 5 and Table 1). Some causative faults, such as the Longmenshan fault of the Wenchuan 8.0 event, are a part of the active block boundaries. Therefore, these earthquakes are linked by regional fields[33] rather than structures.

With 102.5°E as their common boundary, eastern China has quite a different geodynamic condition from western China. Crustal movement, rotational direction, crustal stress, strain field, and structural characteristic all have a clear distinction between eastern and western China, but this did not affect the formation of the linear earthquake sequence that passed through both from west to east.

Correspondingly, the infrared anomaly indicating an earthquake sequence could also extend across different crustal blocks (Fig. 5). In other words, their distribution, structure, and movement are not determined by geological structures or structural provinces, but by the developmental process of a strong earthquake sequence.

8 First Type of Quake Sequence and the Order of Infrared Warming Zone Appearing

According to the characteristics of seismic activity and TIR anomaly, we can divide quake sequences into at least two types. The previously mentioned Yutian–Ryukyu sequence belongs to the first one. This type is characterized by progressive migration of earthquakes, which can be reflected in the shift, veer, deformation, and temperature structure changes of infrared warming zones. The TIR anomaly changing with a shorter duration used to foreshow the quake-sequence evolving in a longer period. Both the order of appearance and the directional distribution of each TIR warming ellipse correspond with the order and location of the quakes in the sequence.

For example, the above-mentioned shift, veer, and temperature structure changes of the infrared warming zones on March 7, 19, April 6, and May 6 in 2008 indicated four (group) strong events in the Yutian–Ryukyu sequence and its branched chain in a few years. The order of the infrared warming areas changing was consistent with the order of four (group) strong quakes beginning to occur (Table 3 and Fig. 6). The first group was the Yutian–Wenchuan earthquake doublet in 2008; the second was the branched chain, including quakes with M_S 6.4 on April 23, 2008, M_S 6.8 on July 13, 2009, m_B 6.9 on February 18, 2010, and so on; the third, an M_S 7.3 event, occurred in Ryukyu on February 26, 2010; and the fourth Yushu M_S 7.1 event occurred on April 13, 2010. The TIR ellipses that earlier appeared indicated the whole sequence process using just 2 months.

Among the four large earthquakes in the Yutian–Ryukyu sequence, the first three events (Yutian, Wenchuan, and Ryukyu) progressively advanced ESE (Fig. 5). Accordingly, the TIR warming area foreshowing the events also moved consistently ESE (Figs. 3 and 6) and shifted to the east of the Wenchuan epicenter on and after March 19, 2008. When the sequence (chain) reached its ESE endpoint Ryukyu, a new large earthquake would return along Y–R chain and occur at Yushu on the WNW side of the Wenchuan epicenter. Surprisingly, the infrared warming ellipses (May 06, 2008) reflecting the relationship between Yushu quake and the chain also made an exception to move back and to stretch across the WNW and ESE sides of the Wenchuan epicenter (Figs. 4 and 6).

Table 3 Ordering relationship between quake-related warming areas and earthquakes.

Alteration of TIR warming area				Occurrence of earthquakes		
Order	Date	Ws	Extension direction	Date	Magnitudes (M_S)	Order
1	March 07, 2008	WNW	ESE	March 20, 2008	7.3	1
2	March 19, 2008	ESE	NNE	April 23, 2008	6.4	2
3	April 06, 2008	ESE	ESE	February 26, 2010	7.3	3
4	May 06, 2008	NE	ESE	April 13, 2010	7.1	4

Notes: If the strong quakes in a group are numerous, then the table lists only the earliest or representative one; Ws indicates that the TIR warming areas were on different sides of the Wenchuan epicenter.

9 Second Type of Quake Sequence

The second is a sequence in which strong earthquakes can alternately occur at two points (small areas); it can be directly reflected in an isolated warming ellipse or belt. The migration direction or track, location, and distribution range of prospective strong earthquakes are legible in a TIR image. The following will analyze a specific example.

The Taiwan region and its northeast had a purple (purple shows the maximum brightness temperature in the image) narrow irregular oval zone in a TIR image on September 9, 1994 (Fig. 7). An M_S 7.2 event (22.52°N, 118.67°E) on September 16, 1994, was just located at the SW end of the ellipse (Fig. 7). Clearly, the purple warming ellipse correlated with the earthquake. But not only that, the ellipse was also an indication of a strong earthquake sequence. The zonal ellipse extended northeastward from Taiwan and contained some linear structural elements with a NE trend. It indicated that the next chained strong earthquakes would occur at the NE end of the ellipse. Sure enough, on January 16, 1995, near Honshu, Japan (34.63°N, 135.02°E), an M_S 7.3 event was just located at the NE end of the ellipse (T-H sequence for short; Fig. 7). Since then, strong earthquakes continued to occur alternately at both ends of the ellipse (Fig. 7 and Table 4).

The earthquakes in Table 4 were mainly located at both ends of the highest warming area. If the quakes occurring in the second highest warming area (bistre in Fig. 7) around the highest one also is counted in, besides in the highest one, then the number of strong earthquakes and the frequency of earthquake migration will increase. The earthquakes in Table 4 are listed up to September 2004. After this, strong earthquakes still occurred at both ends of the chain such as two M_S 6.6 quakes at the NE end (35.35°N, 140.70°E) of the TIR warming zone on April 11, 2011.

The shape of the infrared warming area was, in general, a strip with a NE trending, but not very regular. It can be seen as an aggregation of the chains with same trending, different lengths, and different active periods. The boundaries of the local small areas with lower temperature within the warming area as well as the SW and NE ends of the whole TIR warming area were possible positions where chained strong quakes would occur. For example, the M_S 6.5

Table 4 The strong earthquakes ($M \geq 6.5$) in the T-H sequence from September 1994 to September 2004.

No.	Date	Latitude (deg)	Longitude (deg)	Magnitude	EN	Energy released (10^{15} joule)
1	September 16, 1994	22.52	118.67	7.2	1	3.9811
2	January 16, 1995	34.63	135.02	7.3	1	5.6368
3	February 23, 1995 to September 05, 1996	21.94 to 24.17	121.47 to 122.36	6.5 to 7.0	3	3.2441
4	October 19, 1996 to May 13, 1997	31.71 to 31.94	130.25 to 131.75	6.5 to 7.1	4	4.5280
5	September 20, 1999 to June 10, 2000	23.60 to 24.13	120.67 to 121.30	6.5 to 7.4	8	14.3309
6	July 01, 2000 to March 24, 2001	33.81 to 35.35	133.05 to 139.78	6.6 to 7.2	4	7.3073
7	December 18, 2001 to May 15, 2002	23.37 to 24.92	121.65 to 124.13	6.6 to 7.5	4	22.4830
8	May 26, 2003 to October 31, 2003	37.84 to 38.74	141.56 to 142.23	7.0 to 7.1	2	4.8136
9	December 10, 2003 to May 19, 2004	22.83 to 23.01	121.37 to 121.51	6.5 to 6.9	2	1.7674
10	September 05, 2004 to September 06, 2004	33.02 to 33.15	136.94 to 137.50	6.5 to 7.4	3	13.9215

Notes: According to CSN earthquake catalog; EN means the number of earthquakes.

event (25.90°N, 129.76°E) on May 26, 2010, and the M_S 6.6 event (35.35°N, 140.70°E) on April 11, 2011, were at both ends of a shorter chain; from the M_S 7.2 event (22.52°N, 118.67°E) on September 16, 1994, to the M_S 7.3 event (34.63°N, 135.02°E) on January 16, 1995, was a migration along a long chain (Fig. 7).

The release of quake energy was more uniform at both ends of the sequence (chain) in the first 3 years. After that, in different stages, seismic activity was more intense at one end (SW or NE) of the chain than at the other end (Table 4).

The TIR warming areas indicating such an earthquake sequence have better directionality of the overall shape and internal structure. Strong earthquakes tend to occur at the ends or boundary's inflexions of the whole warming area, secondary temperature structures, and the inner small areas with exceptional temperature alteration.

10 Composite Earthquake Sequences

Close to the east of the Yutian–Ryukyu sequence, there was a strong quake sequence (chain) roughly extending in the NE direction which has a larger range, intensity, and frequency of seismic activity (mainly on the east of the line connecting the two epicenters of 2004 M_W 9.3 and 2011 M_W 9.0). The respective distribution, orientation, and structural characteristics of the two sequences and their relationship were clearly reflected in a TIR image on December 10, 2004 (Fig. 8).

From Fig. 8, we can see that the TIR warming area had two sets of structures with different shapes and orientations. One was located in the east of the image, and its warming area strikes were NE taking the shape of the triangle whose north end is narrower and whose south end is wider. The smaller TIR belts with brightness temperatures more than 294 K, from 294 to 284 K, from 283 to 276 K, and from 275 to 254 K within the triangle also extended in the NE direction. The other TIR structure was in the west and middle of the image, along the Yutian–Ryukyu sequence with a strike ESE that was slightly curved. It was a warming broadband whose main part was under the Y–R chain. The internal secondary TIR linear structures were in the ESE direction near the Y–R chain, the EW direction near 25°N, and the NE direction to the south of 25°N, showing a trend of converging at the N-terminal of the triangular sequence and a connection with the triangular sequence. The eastern end of this sequence was intercepted by the triangular sequence. At the intersection of the two sequences in the Ryukyu Islands, an M_S 7.3 quake occurred on February 26, 2010.

Large numbers of strong quakes alternately occurred at both ends of the triangle chain with a NE strike. In a short period of 7 years, about 60 $M \geq 7$ earthquakes occurred there and both ends of the chain had $M_W \geq 9.0$ events (Table 5 and Fig. 8). Activity of strong earthquakes in the SW end of the triangle chain was more intense than in the NE end except around March 2011 when the Japan M_W 9.0 quake occurred. This could be reflected in the duration, magnitude, and frequency of seismic activity (Table 5).

11 Significance of Studying the Infrared Indication of Earthquake Sequences

1. TIR images can validate a quake sequence's existence and show its distribution, development, and structural relationship.
2. It can be used to analyze the possibility and location of subsequent strong earthquakes.
3. When people analyzed seismic activity, they used to divide strong quakes into different periods and episodes. This partition was mainly based on earthquake zones, tectonic systems, and seismicity. Our research considers, however, that a quake's occurrence can affect or trigger quakes in other tectonic belts or blocks due to the interaction between crustal blocks. Some potential links make these blocks all in a scope of stress redistribution after a seismic stress release. There were many examples that an earthquake spanned blocks to remotely trigger other earthquakes. The correlation between earthquakes is determined jointly by stress sources, structures, movements, and contacting relationships of crustal blocks. This complex correlation, however, can be intuitively shown in infrared images because TIR warming areas are a direct reflection of the fields gestating earthquakes. TIR offers a new way to divide the regions where strong quakes possibly interact and to analyze earthquake activity periods in the regions.

Table 5 Strong earthquakes ($M \geq 7$) activities in the triangle chain.

No.	Location in the chain	Start of seismic activity	Duration (days)	Magnitude (M_S)	Seismic frequency	*Ing* (days)
1	S end	December 26, 2004	6	7.1 to 9.3 (M_W)	4	18
2	N end	January 19, 2005	1	7	1	38
3	S end	February 26, 2005	1	7	1	22
4	N end	March 20, 2005	1	7.3	1	8
5	S end	March 28, 2005	99	7.0 to 8.6	6	32
6	N end	August 16, 2005	90	7.2 to 7.3	2	181
7	S end	May 16, 2006	62	7.3 to 7.4	2	162
8	Middle part	December 26, 2006	1	7.1 to 7.4	2	89
9	N end	March 25, 2007	113	7.0 to 7.2	2	23
10	S end	August 08, 2007	201	7.1 to 8.6	8	72
11	N end	May 07, 2008	127	7.0 (m_B) to 7.3	5	66
12	S end	November 16, 2008	87	7.0 to 7.4	2	179
13	N end	August 09, 2009	1	7.1 (m_B)	1	7
14	S end	August 16, 2009	46	7.0 to 7.6	4	147
15	Middle part	February 26, 2010	1	7.3	1	7
16	S end	March 05, 2010	234	7.0 to 7.9	6	57
17	N end	December 21, 2010	201	7.0 to 9.0 (M_W)	8	121
18	Middle part	November 18, 2011	1	7.2 (m_B)	1	63
19	S end	January 10, 2012	1	7.2	1	64
20	N end	March 14, 2012	1	7.2	1	28

Notes: This is the result of analyzing the data of the CSN earthquake catalog from December 2004 to March 2012; *Ing* is the time interval between the seismic activity in this group and in next group.

For instance, the quakes in the Yutian–Ryukyu sequence had an approximately symmetrical structure of spatial and temporal distributions. It reveals a transcontinental broad zone from the West Kunlun to the Ryukyu Islands, in which seismic preparation and occurrence has a stage characteristic, and the seismogenic units have an interaction in near east-west direction. Without discernible link relations of earthquakes, getting such cognition is very difficult. From April 23, 2008, to November 8, 2011, eight quakes with magnitudes 6.0 to 7.2 occurred in the area (latitude 22.96°N to 27.20°N, longitude 120.70°E to 125.90°E) where the Yutian–Ryukyu sequence passing through (Fig. 3 and Table 2). From the TIR images' analysis above, we can determine that those events do not belong to the Yutian–Ryukyu sequence and instead belong to a branched chain. If those quakes are mistakenly assumed to belong to the Yutian–Ryukyu sequence, then the real correlation between the quakes will be covered up, that neither temporal pattern of seismicity nor the spatial extent where seismic processes are related to each other can be correctly understood.

12 Conclusion

Earthquake sequences have at least two types: (1) quakes progressively migrating along a certain direction and that move back from the end of the route; (2) quakes alternately occurring at both ends of a long and narrow zone. Both types can meet and form a more complex chain structure.

All the strong quake sequences can traverse different tectonic blocks or systems. They can be clearly and intuitively foreshowed by TIR images with abnormal brightness temperature changes that are independent of topographies and geological structures. The signs indicating the sequences usually manifest as the shift, veer, deformation, and temperature structure changes of TIR anomaly areas or a long and narrow isolated warming structure with obvious directional characteristics. The short-term changes of TIR anomalies can indicate the longer developing process of a strong earthquake sequence. By their configuration, orientation, location, temperature relationship, structural elements, and variation in these aspects, the TIR signs can be found a few years prior to the formation of a sequence. Furthermore, the TIR anomaly zone can link up quakes with preparation processes that are closely related, so TIR images can be used to outline the area in which seismicity follows some uniform spatiotemporal rules.

References

1. C. J. Ammon, H. Kanamori, and T. Lay, "A great earthquake doublet and seismic stress transfer cycle in the central Kuril islands," *Nature* **451**, 561–565 (2008).
2. J. Deng and L. R. Sykes, "Triggering of 1812 Santa Barbara earthquake by a great San Andreas shock: implications for future seismic hazards in southern California," *Geophys. Res. Lett.* **23**(10), 1155–1158 (1996).
3. Z. Duputel et al., "The 2012 Sumatra great earthquake sequence," *Earth Planet. Sci. Lett.* **351–352**, 247–257 (2012).
4. A. M. Freed and J. Lin, "Delayed triggering of the 1999 Hector Mine earthquake by viscoelastic stress transfer," *Nature* **411**, 180–183 (2001).
5. S. J. Gibowicz and S. Lasocki, "Analysis of shallow and deep earthquake doublets in the Fiji-Tonga-Kermadec region," *Pure. Appl. Geophys.* **164**(1), 53–74 (2007).
6. J. Gomberg et al., "Earthquake nucleation by transient deformations caused by the $M = 7.9$ Denali, Alaska, earthquake," *Nature* **427**, 621–624 (2004).
7. J. Gomberg and P. Johnson, "Seismology: dynamic triggering of earthquakes," *Nature* **437**, 830 (2005).
8. J. Gomberg et al., "Earthquake triggering by seismic waves following the Landers and Hector Mine earthquakes," *Nature* **411**, 462–466 (2001).
9. R. A. Harris, R. W. Simpson, and P. A. Reasenberg, "Influence of static stress changes on earthquake locations in southern California," *Nature* **375**, 221–224 (1995).
10. E. A. Jagla, "Delayed dynamic triggering of earthquakes: evidence from a statistical model of seismicity," *Europhys. Lett.* **93**(1), 1–6 (2011).
11. Y. Y. Kagan and D. D. Jackson, "Worldwide doublets of large shallow earthquakes," *Bull. Seismol. Soc. Am.* **89**(5), 1147–1155 (1999).
12. G. C. P. King, R. S. Stein, and J. Lin, "Static stress changes and the triggering of earthquakes," *Bull. Seismol. Soc. Am.* **84**(3), 935–953 (1994).
13. T. Lay and H. Kanamori, "Earthquake doublets in the Solomon Islands," *Phys. Earth Planet. Inter.* **21**(4), 283–304 (1980).
14. T. Lay et al., "The 2006–2007 Kuril Islands great earthquake sequence," *J. Geophys. Res.* **114**(B11), B11308 (2009).
15. A. Nur, H. Ron, and G. C. Beroza, "The nature of the Landers-Mojave earthquake line," *Science* **261**, 201–203 (1993).
16. R. S. Stein, J. H. Dieterich, and A. A. Barka, "Role of stress triggering in earthquake migration on the North Anatolian Fault," *Phys. Chem. Earth* **21**(4), 225–230 (1996).
17. R. S. Stein, G. C. P. King, and J. Lin, "Change in failure stress on the southern San Andreas fault system caused by the 1992 magnitude = 7.4 Landers earthquake," *Science* **258**, 1328–1332 (1992).
18. M. Wyss and S. Wiemer, "Change in the probability for earthquakes in Southern California due to the Landers magnitude 7.3 earthquake," *Science* **290**, 1334–1338 (2000).
19. R. Tibi, D. A. Wiens, and H. Inoue, "Remote triggering of deep earthquakes in the 2002 Tonga sequences," *Nature* **424**, 921–925 (2003).
20. M. Reyners, D. Eberhart-Phillips, and S. Martin, "Prolonged Canterbury earthquake sequence linked to widespread weakening of strong crust," *Nat. Geosci.* **7**, 34–37 (2014).

21. Z. J. Qiang et al., "Satellitic thermal infrared brightness temperature anomaly image: short-term and impending earthquake precursors," *Sci. China Ser. D: Earth Sci.* **42**(3), 313–324 (1999).
22. Z. J. Qiang, "Monitoring and predicting impending earthquakes using satellite remote sensing technique," in *Report of the United Nations/ESCAP/UNDRC Workshop on the Application of space techniques to combat nature disasters*, pp. 102–108, Bangkok, Thailand (1991).
23. Z. J. Qiang, X. D. Xu, and C. G. Dian, "Case 27 thermal infrared anomaly precursor of impending earthquakes," *Pure Appl. Geophys.* **149**(1), 159–171 (1997).
24. Q. L. Yao and Z. J. Qiang, "The elliptic stress thermal field prior to M_S 7.3 Yutian, and M_S 8.0 Wenchuan earthquakes in China in 2008," *Nat. Hazards* **54**(2), 307–322 (2010).
25. Q. L. Yao and Z. J. Qiang, "Thermal infrared anomalies as a precursor of strong earthquakes in the distant future," *Nat. Hazards* **62**(3), 991–1003 (2012).
26. CNN Library, "2011 Japan Earthquake—Tsunami Fast Facts," http://edition.cnn.com/2013/07/17/world/asia/japan-earthquake---tsunami-fast-facts/ (11 July 2014).
27. H. S. Srivastava et al., "Comparative evaluation of potential of optical and SAR data for the detection of human settlements using digital classification," *Int. J. Geoinf.* **2**(3), 21–28 (2006).
28. H. S. Srivastava, P. Patel, and R. R. Navalgund, "Application potentials of synthetic aperture radar interferometry for land-cover mapping and crop-height estimation," *Curr. Sci.* **91**(6), 783–788 (2006).
29. A. Favretto, R. Geletti, and D. Civile, "Remote sensing as a preliminary analysis for the detection of active tectonic structures: an application to the Albanian orogenic system," *Geoadria* **18**(2), 97–111 (2013).
30. L. Dong and J. Shan, "A comprehensive review of earthquake-induced building damage detection with remote sensing techniques," *ISPRS J. Photogramm.* **84**, 85–99 (2013).
31. A. Ajmar, P. Boccardo, and F. G. Tonolo1, "Earthquake damage assessment based on remote sensing data. The Haiti case study," *Ital. J. Remote Sens.* **43**(2), 123–128 (2011).
32. Q. L. Yao, "Influence of regional earthquake on flood in mainland China," *Meteorol. Disaster Reduct. Res.* **31**(4), 34–42 (2008).
33. Q. L. Yao, "Field effect and regional conversion as the mechanism of natural hazard chains," *Meteorol. Disaster Reduct. Res.* **30**(3), 31–36 (2007).

Qinglin Yao received his MS degrees in seismology and geology from the University of Science and Technology of China in 1986. He has been working at the Institute of Geology, China Earthquake Administration since then, and he is currently a professor. His research focuses on seismic infrared precursors that are identified by satellite remote sensing images and tectonics, but he also does research on hazard chain, risk analysis, and some optimal algorithms of hazard mitigation system.

Zuji Qiang received his Kandidat Nauk (doctorate) from Moscow State University in 1961. From 1977, he was a researcher of tectonics and earthquake forecast at the State Seismological Bureau, and he is currently a professor. Since 1989, he and his group have explored seismic short-impending prediction by satellite remote sensing images reflecting abnormal warming, and their studies were praised by the Chinese State Science and Technology Commission, the State Remote Sensing Center, and the State Seismological Bureau.